Mixtures of Tertiary Amine-Functionalized Mesogens with Poly(acrylic acid)

Amir Tork and C. Geraldine Bazuin*

Centre de Recherche en Sciences et Ingénierie des Macromolécules (CERSIM), Département de Chimie, Université Laval, Québec, Canada G1K 7P4

Received April 9, 2001; Revised Manuscript Received July 5, 2001

ABSTRACT: Diethylamine-functionalized alkoxy methoxy biphenyl mesogens of variable spacer lengths (LC-1,*n*N, $n = 5-12$) and their equimolar mixtures with poly(acrylic acid) (PAA) were investigated by infrared spectroscopy, differential scanning calorimetry, polarizing optical microscopy, and X-ray diffraction. The pure LC-1,*n*N are polymorphic, generally possessing two different crystalline phases [a (full or partial) bilayer at ambient temperature followed by an orthogonal monolayer at higher temperatures], whose detailed characteristics depend on the spacer length. The mesogen melting point (a lamellar E-like−isotropic transition) is independent of spacer length. The equimolar LC-1,*n*N/PAA mixtures are biphasic, composed of a mesogen-pure phase and a phase composed of a polymer−mesogen complex resulting from proton-transfer interactions. The former is unperturbed by the presence of the latter. The complexes are liquid crystalline, most likely in the form of a partial or interdigitated smectic A mesophase. The smectic−isotropic transition temperatures are generally higher than the mesogen melting points and increase strongly with spacer length.

Introduction

It has become well-established within the past decade that supramolecular liquid crystalline polymers (LCPs) can be easily designed by the self-assembly of appropriately functionalized molecular constituents.[1−3] The self-assembly process is generally based on attractive interactions between complementary functional groups, leading, for example, to directed hydrogen bonding, acid−base interactions, or oppositely charged ionic interactions. Both main-chain[4,5] and side-chain supramolecular LCPs have been designed. The latter have received the greatest attention, with notable examples comprising an extensive series, developed by Kato and Fréchet and colleagues,[6] that are based on hydrogen-bonding interactions between (small-molecule) pyridyl and (polymeric) benzoic acid functionalities located far from the polymer backbone.

Various other researchers have studied side-chain supramolecular systems where the interaction site is near the polymer backbone, allowing the use of simple, readily available polymers. Such systems include a wide variety of common surfactant/polyelectrolyte complexes usually based on hydrogen-bonding[7] or ionic[8−11] interactions. A smaller number of complexes have been reported where a thermotropic mesogenic moiety forms part of the surfactant molecule.[12−15] These types of molecules have special interest in that the often well-separated polar (or ionic) and mesogenic moieties can both influence the liquid crystalline characteristics, possibly antagonistically or synergistically.

We have previously communicated[13] that a disordered liquid crystalline mesophase can be generated by the complexation of simple acidic polymers such as poly(acrylic acid) (PAA) or sulfonated polymers with amine- or ammonium-functionalized mesogens, none of which individually possess such mesophases. In this paper we present a detailed thermal and structural investigation of equimolar mixtures of PAA and diethylamine-functionalized mesogens of variable alkyl spacer lengths (shown in Chart 1). The mesogens are given the nomenclature, LC-1,*n*N, where *n* refers to the number of carbons, from 5 to 12, in the spacer (the first number refers to the single carbon in the tail and N to the amine functionality). A comparable system reported in the literature is that of Tal'roze et al.[14] where two different dimethylamine-functionalized small molecules with a very short alkyl spacer (two methylene units) and a (short) mesogen-like core possessing a long alkyl tail are complexed with PAA and poly(methacrylic acid). These systems are characterized by (hydrogen-bonded) ionic complexation caused by proton-transfer interactions between the constituents. The present study will show how the characteristics of the system depend on spacer length, and some comparisons will be made regarding the size of the amine function employed (diethyl vs dimethyl). The focus on stoichiometric mixtures, which as will be shown are biphasic, allows the investigation of both coexisting phases and is of interest in that biphasic systems can be more advantageous for some applications than monophasic ones.[16]

Chart 1

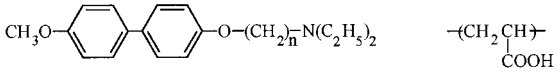

LC-1,*n*N (n = 5-12) PAA

Experimental Part

Synthesis of LC-1,*n*N and Preparation of the LC-1,*n*N/PAA Mixtures. The synthesis of LC-1,*n*N was accomplished in three main steps whose details are described in the Supporting Information: first a methoxy tail and then a bromine-terminated alkyl spacer were fixed to opposite ends of a biphenyl core, and last, the bromine was replaced by a tertiary amine moiety. PAA in powder form, obtained from Aldrich and reported to have a molar mass (M_w) of 250000, was generally used as received (initially, it was precipitated into 2-propanol from a concentrated aqueous solution, but since this procedure was not observed to affect the data obtained, it was subsequently abandoned).

Unless otherwise indicated, the mixtures were prepared in anhydrous ethanol (Commercial Alcohols), used as received.

10.1021/ma010607f CCC: $20.00
Published on Web 10/16/2001

First, the accurately weighed components were dissolved separately in hot ethanol (about 70 °C), giving transparent solutions. After the solutions were stirred for at least 30 min, the LC-1,*n*N solution was added all at once to the PAA solution, followed by rinsing, to give a final solution of about 1% concentration. A very fine precipitate formed immediately, giving a slightly cloudy solution even at reflux; this behavior is indicative of complexation between the two components in solution and was also observed by Kornienko et al.[17] for the comparable system mentioned in the Introduction.[14] The solution was stirred for 12 h at 40 °C with little change in appearance. After evaporation of the solvent at ambient temperature, the resulting product was finely ground, and then further dried in vacuo usually at about 45 °C for 2 weeks and sometimes at 70 °C for 4 days (there were no observable differences in the results obtained for the two drying conditions). All dried powders were cream-colored. Other solvents (for example, 50:50, v/v, THF/H_2O and 90:10, v/v, pyridine/H_2O, which remained transparent when the LC-1,*n*N and PAA solutions were mixed) were found to be equally effective in preparing the LC-1,*n*N/PAA mixtures, but were not used systematically.

Techniques of Analysis. Differential scanning calorimetry (DSC) was performed with Perkin-Elmer DSC-4 and DSC-7 calorimeters, calibrated with indium and flushed with helium. About 10 mg of sample was packed into standard aluminum pans, and scanned at heating and cooling rates of 5 °C/min. For the mixtures with PAA, the runs were limited to a maximum temperature of 135 °C whenever possible, to avoid anhydride formation between acid groups that takes place at higher temperatures.[18−20] First-order transition temperatures are given by the peak values, and glass transitions by the midpoint of the heat capacity jump.

Polarizing optical microscopy (POM) was performed using a Zeiss Axioskop microscope, equipped with a 25X Leica objective, a 35 mm Yashica camera, a Mettler FP52 hotplate, and a FP5 temperature controller. Scanning electron micrographs were obtained with a JEOL JSM-840A instrument, with the sample glued to an aluminum stub and coated with a very thin layer of Pd/Au alloy.

X-ray diffraction studies were carried out with a Rigaku rotating anode (Rotaflex RU-200BH), operated at 50−55 kV and 190 mA, using Ni-filtered Cu Kα (1.542 Å) radiation. Two sets of data encompassing the wide angles were obtained, one ($2\theta = 2.2-40°$) requiring relatively short exposure times (about 1 h) and the other ($2\theta = 1.1-35°$) requiring very long exposure times (up to 5 h). Because of the long exposure times, the latter measurements were restricted to a limited number of temperatures and samples. Collimation was achieved using a Soller slit, along with a 2 mm pinhole for the former and a 1 mm pinhole for the latter. Small-angle data ($2\theta = 0.15-7°$) were obtained using a beam collimated by two slits of widths 0.16 and 0.12 mm, respectively; the sample-to-detector distance was 200 mm. For both wide and small angles, a scintillation counter coupled to a pulse-height analyzer served as detector, which at small angles was fitted to a camera under vacuum. The temperature was controlled by a homemade water-cooled copper block oven. Powdered samples were packed into 1.5 mm diameter Lindemann capillary tubes (Charles Supper Co.). The Bragg spacings determined from the small-angle X-ray data were compared with calculated molecular lengths as obtained from Hyperchem (Hypercube) and CPK models, assuming most extended conformations and including van der Waals radii at the extremities.

Fourier transform infrared (FTIR) spectra were obtained from an accumulation of 100 interferograms at a resolution of 4 cm^{-1}, using a Mattson Sirius 100 FTIR spectrometer equipped with a mercury−cadmium−tellurium detector. All samples, including pure PAA, were prepared by grinding well-ground dried powder with dried KBr, and compressing the powder into pellets; the pellets were stored in a desiccator until use.

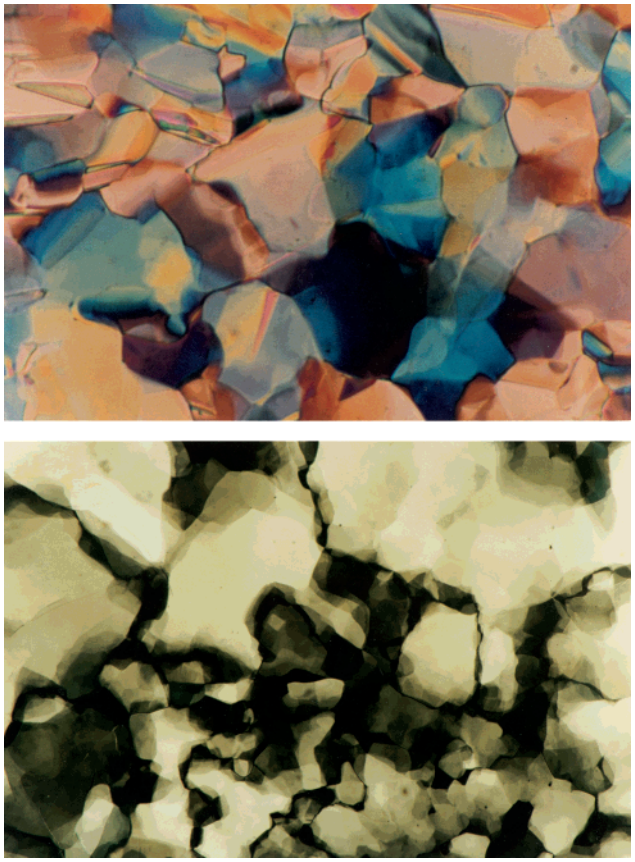

Figure 1. Polarizing optical micrographs of (a, top) LC-1,5N and (b, bottom) LC-1,10N, obtained at 50 °C after cooling from the isotropic phase.

Results

Functionalized Mesogens. DSC and POM observations indicate that all members of the LC-1,*n*N series melt from an ordered or crystalline phase directly into the isotropic[21] phase at 79 ± 3 °C on heating and 75 ± 4 °C on cooling.[22] Evidently, there is little dependence of the transition temperature on alkyl spacer length [in comparison, the Br-terminated precursors that were tested have higher melting points (crystal-to-isotropic transitions) that do depend on the spacer length: 89 °C (ΔH, 70 J/g) and 120 °C (ΔH, 150 J/g) for $n = 9$ and 12, respectively[23]]. POM textures of the ordered phase, shown in Figure 1 for a short and a long spacer, respectively, are reminiscent of the platelet texture of the crystal E mesophase[24] illustrated in ref 25. This assignment would be consistent with the small supercooling observed for the transition, noting also that a crystal E or E-like[26] phase is frequently obtained for 4,4′-disubstituted biphenyl mesogens.[27−30]

One or more minor transitions are also apparent in the DSC thermograms at 5−20 °C below the melting point or major transition (with the exact number and temperatures appearing to be sensitive to thermal and sample history): for $n = 5-9$ they are present in both heating and cooling thermograms, for $n = 10$ and 11 they are present in the cooling thermograms only, and for $n = 12$ none are visible. Strikingly, in the presence of a minor transition, the enthalpy of the melting point is generally constant at about 16 kJ/mol. This independence of the melt enthalpy on spacer length suggests that the melting point is dominated by thermodynamic changes involving interactions of the rigid biphenyl core

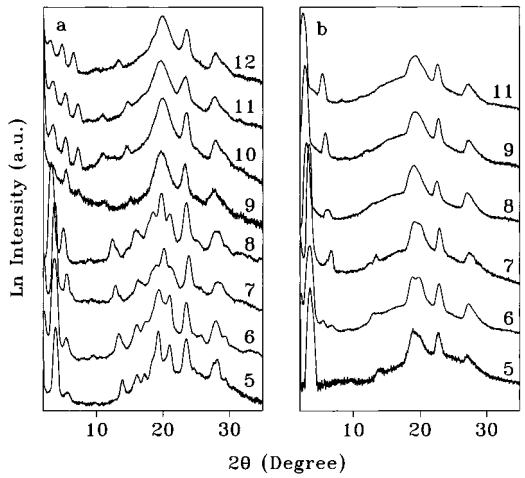

Figure 2. Wide-angle X-ray diffractograms of the LC-1,*n*N with *n* indicated for each curve: (a) at ambient temperature, (b) in the higher temperature phase ($n = 10$ is not included in the latter because the available trace could not be converted successfully to ln form).

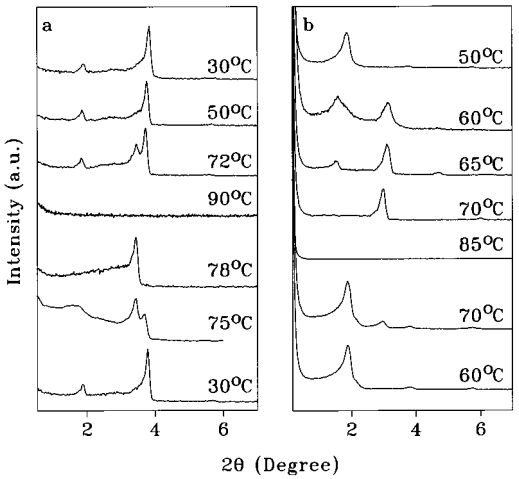

Figure 3. Small-angle X-ray profiles of (a) LC-1,6N and (b) LC-1,9N at the nominal temperatures indicated, taken in order from the bottom to top of the figure.

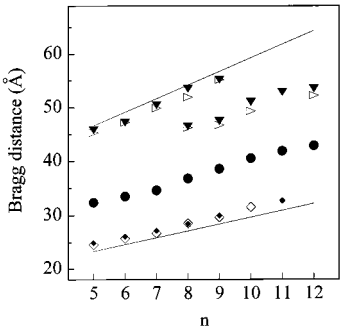

Figure 4. Bragg distances as a function of *n* for LC-1,*n*N (open symbols) and equimolar LC-1,*n*N/PAA mixtures (filled symbols): triangles, ambient temperature phase; tilted squares, higher temperature phase; circles, liquid crystalline phase. The lines connect the values calculated for *l* and 2*l*, where *l* is the calculated molecular length of LC-1,*n*N in extended conformation.

and not the alkyl chains. In contrast, in the absence of a minor transition, the melt enthalpy increases with spacer length up to 32 kJ/mol, implying that the processes occurring in the minor and major transitions now occur simultaneously and involve the alkyl chains. It may be concluded that the alkyl chains are not in a crystalline state between the minor and major transitions (although they may remain extended), and are possibly only partially crystalline at lower temperatures. Such partial disorder can be related to the difference in cross-sectional area between the large diethylamine function and the (extended) alkyl spacer and biphenyl moiety.

In accordance with the DSC data, two distinct sets of X-ray profiles are obtained below (Figure 2a) and above (Figure 2b) the minor transitions—noting that the latter are obtained on cooling only for $n = 10$ and 11, and that the profiles of $n = 12$ have the same form at all temperatures below the major transition. Furthermore, the ambient temperature profiles for the shorter mesogens are distinct from those for the longer mesogens (Figure 2a), whereas above the minor transition the profiles are similar for all of the mesogens (Figure 2b).

In the wide-angle region, patterns resembling those for E-like mesophases[27−30] are observed for $n = 12$, for $n = 9-11$ both below and above the minor transitions, and for $n = 5-8$ above the minor transitions (in some cases, the diffraction peak near $2\theta = 20°$ appears to be decomposed into two peaks, although the total width is similar for all). On the other hand, for $n = 5-8$ at ambient temperature, there are a greater number of wide-angle diffraction peaks, indicative of a more highly ordered phase (the details appear to be sensitive to sample history, consistent with the sensitivity noted above for the minor DSC transition). These data indicate that the minor transitions involve significant changes in short-range order for the shorter mesogens, but not for the longer mesogens.

The lower angle region indicates that the ordered phases of all mesogens are lamellar in nature (as would be expected for E phases). This is shown at ambient temperature for $n = 9-12$ by the presence of four small-angle diffraction peaks with reciprocal spacings in the ratio 1:2:3:4 and for $n = 5-8$ by three peaks in the ratio 1:2:3 (note that the first-order reflection is observed only in the small-angle data, shown in Figure 3 for $n = 6$ and 9). It is noteworthy that it is the second-order reflection that is the most intense in the case of the shorter mesogens, which may be related to an additional plane of symmetry in their lamellar electron density profile.[29] In the higher temperature phase, there are two small-angle reflections with reciprocal spacings in a 1:2 ratio, also consistent with a lamellar structure [Figure 2b for $n = 5-11$, and Figures 3a (78 °C curve) and 3b (middle curve) for $n = 6$ and 9, respectively]. Some of the profiles in Figure 3 show an overlap of the diffraction peaks of the ambient and higher temperature phases (due to imperfect temperature control), thus clearly demonstrating that they are two separate phases with distinct lamellar spacings.[31]

The lamellar spacings, *d*, obtained from the SAXS data by application of the Bragg equation to the lowest angle peak of each phase for each mesogen are plotted as a function of the spacer length, *n*, in Figure 4 (open symbols), and compared with the calculated molecular lengths, *l* and 2*l* (representing orthogonal monolayer and bilayer phases, respectively), of the mesogens in their most extended conformations. The slopes of the Bragg distances as a function of *n* as well as their extrapolated values at $n = 0$ are given in Table 1. It is observed that the lamellar thickness of the higher temperature phase is similar to a single molecular length ($d/l = 1.05 \pm 0.02$), and increases linearly with

Table 1. Intercepts ($n = 0$) and Slopes of the Bragg Distance versus n Plots[a]

	LC-1,*n*N		LC-1,*n*N/PAA	
phase	intercept (Å)	slope (Å/CH_2)	intercept (Å)	slope (Å/CH_2)
ambient temperature[b] (shorter mesogens)	34 ± 1	2.4 ± 0.2	33 ± 1	2.5 ± 0.2
ambient temperature (longer mesogens)	32 ± 3	1.8 ± 0.2	34 ± 4	1.6 ± 0.3
higher temperature	17 ± 1	1.4 ± 0.1	18 ± 1	1.3 ± 0.1
liquid crystalline[c]			25 ± 2	1.4 ± 0.2

[a] The uncertainties given include measurements on different preparations of the same sample in several cases. [b] The Bragg distances obtained for $n = 9$ for the phase detected between its higher temperature and ambient temperature phases are included in the data. [c] The uncertainties given include the different values obtained by the choice of Bragg distances used (based on the second-order reflection for all n, based on the first-order reflection for $n = 8-12$ only, based on the second-order reflection for $n = 5-7$ plus the first-order reflection for $n = 8-12$, and based on the second-order reflection for all n as detected at ambient temperature).

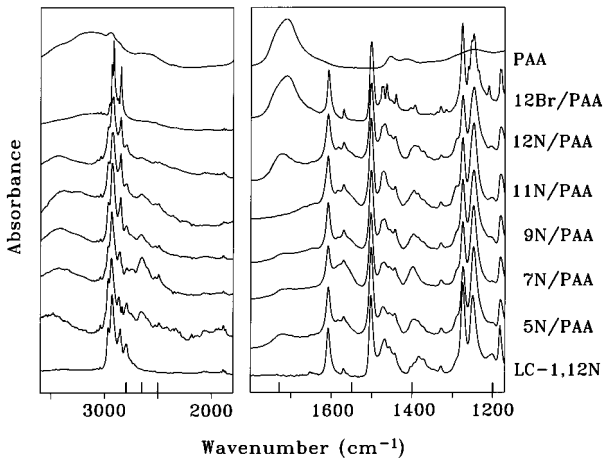

Figure 5. FTIR spectra of PAA, an equimolar LC-1,12Br/PAA mixture, representative equimolar LC-1,*n*N/PAA mixtures, and LC-1,12N. The lines at the bottom of the figure pinpoint the principal bands referred to in the text.

n at about 1.4 Å/CH_2. The extrapolated spacing of 17 Å at $n = 0$ is consistent with that estimated from molecular models for the combined lengths of the methoxy, biphenyloxy, and diethylamine moieties. These data and the wide-angle results indicate that the higher temperature phase is an orthogonal E-like monolayer phase.

The lamellar thickness of the ambient temperature phase corresponds to almost two molecular lengths for the shorter mesogens ($d/l = 1.93 \pm 0.01$), but is significantly less for the longer mesogens ($d/l = 1.66 \pm 0.04$), with corresponding slopes of about 2.4 and 1.8 Å/CH_2, respectively. The former is indicative of an orthogonal bilayer phase, whereas the latter must involve some interdigitation of the molecules in an orthogonal phase (partial bilayer) or possibly tilting of the mesogenic long axis relative to the layer normal (tilted bilayer). Extrapolation of the Bragg spacings to $n = 0$ gives a similar value of about 33 Å for both the shorter and longer mesogens (although with greater uncertainty for the latter, Table 1), which is about twice that obtained for the single-layer higher temperature phase. This suggests that the biphenyl core and polar headgroups are arranged similarly—i.e., in orthogonal fashion—for all of the mesogens at ambient temperature. For the longer mesogens, this would also be consistent with the E-like phase suggested by the wide-angle data. A similar phenomenon distinguishing shorter and longer alkyl chain lengths was observed by Ujiie et al.[32] in supramolecular complexes of poly(ethylenimine) with *n*-alkanoic acids of 6−18 carbons, albeit for a disordered smectic phase; this was explained by a change from an orthogonal to a tilted bilayer.

These mesogens can be compared with the relatively small number of other rodlike mesogens with similar architecture—that is, where a (nonionic) polar group is well separated from an aromatic mesogenic core para-substituted with aliphatic chains—that have been reported in the literature.[33] A notable example is a series of cyano-capped mesogens (4-cyanoalkoxybenzylidene-4′-alkylanilines, with up to eight carbons in the alkyl spacer), where transitions between bilayer and monolayer smectic A phases were observed, and where the second-order X-ray reflection of the bilayer phase is much more intense than the first-order reflection.[34] In carboxylic acid-capped mesogens of the same type as those studied here, a bilayer E-like phase was observed, again with a somewhat smaller d/l ratio for an 11-carbon spacer (LC-1,11A)[35] compared to a 6-carbon spacer (LC-4,6A):[27] $d/l = 1.5$ and 1.8, respectively. These kinds of mesogens without the polar cap generally give single-layer phases.[34] Thus, the polar cap appears to influence the layer thickness in ways reminiscent of polar tails that are directly attached to the mesogenic core.

Mixtures of LC-1,*n*N and PAA. The state of complexation between the components in the stoichiometric LC-1,*n*N/PAA mixtures was qualitatively evaluated by infrared spectroscopic analysis. Ambient temperature spectra of representative mixtures are compared in Figure 5 with those of pure PAA, a pure mesogen, and a stoichiometric LC-1,12Br/PAA mixture (where there is no proton transfer). This figure shows that partial proton transfer from the acid to the amine moieties occurs in the mixtures as anticipated, indicated in particular by the decrease in intensity but not the disappearance of the acid carbonyl absorption in the 1700−1740 cm^{-1} range compared to what is observed in the LC-1,12Br/PAA spectrum (using the biphenyl bands at 1500 and 1600 cm^{-1} as internal standards), and by the appearance in the mixtures of a new, albeit weak and broad, absorption band at about 1550 cm^{-1} attributed to the asymmetric COO^- stretch (on which a weak LC band at 1569 cm^{-1} is superimposed). Changes in the region of the symmetric COO^- stretch region near 1400 cm^{-1} are also evident. In addition, a new weak band near 2650 cm^{-1} and a very weak band near 2500 cm^{-1} generally appear in the LC-1,*n*N/PAA (but not in the LC-1,*n*Br/PAA) mixtures, and may be attributed to the (hydrogen-bonded) protonated amine moiety ($^+HEt_2N-$, $-CO_2^-\cdots{}^+HEt_2N-$). Finally, the ethyl band at 2798 cm^{-1} and a weak C−N band at about 1200 cm^{-1} decrease in intensity in the LC-1,*n*N/PAA mixtures compared to the pure LC-1,*n*N. A weak band at 1585 cm^{-1} in the mixtures may be due to a bending mode of the tertiary amine salt,[36] or it may be related to the asymmetric carboxylate stretch, a mode which is frequently characterized by more than one band.[37] Analogous features were noted[17,38] in the similarly interacting systems of ref 14 involving dimethylamine functionalities.

Regarding the weakness and breadth of the 1550 cm^{-1} band, we have previously observed, in blends of poly-

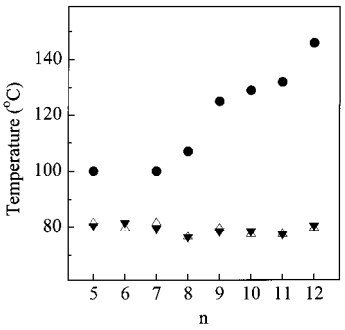

Figure 6. Transition temperatures as a function of *n* for LC-1,*n*N (open symbols) and equimolar LC-1,*n*N/PAA mixtures (filled symbols): triangles, melting point; circles, clearing temperature.

(ethylenimine) and carboxylic acid-functionalized mesogens characterized by extensive proton transfer, that this band is sharp and intense only when there are virtually no acid groups remaining in the system.[39] This was considered to be related, at least in part, to the formation of acid−salt structures when excess acid groups are present as is the case in the present system. If so, the weakness of the 1550 cm^{-1} band is not necessarily indicative of a low extent of proton transfer. Others have suggested that the acid proton is not fully transferred to the amine, resulting in hydrogen bonding with strong proton polarization.[38]

It was noted that the shape and intensity of both the carbonyl and carboxylate absorptions are somewhat variable from one mixture to the next. Although this may be (partly) a result of variable degrees of proton transfer, it may also be related to variability in the local environment of the absorbing species (due, for example, to variable local coordination structures of the carboxylate ions, variable distributions and types of free and dimerized acid groups, variable acid−salt structures, and/or the presence of residual water molecules[39]). In any case, we were unable to find any significant correlation between these features in the infrared spectra and the thermal and structural data.

Quantitative analysis of the carbonyl absorption, which will be reported in detail separately,[40] indicates that proton transfer in the LC-1,*n*N/PAA mixtures occurs to an extent of 40−50%. This can be compared to the 2:1 (acid:amine) stoichiometry proposed by Kornienko et al.[17] for complexes of PAA with *β*-*N*-dimethylamino-4-dodecyloxypropiophenone. Thus, the diethyl- and dimethylamino moieties appear to react similarly with PAA, despite the differences in their bulkiness. It may be added that we observed no drastic changes in the spectra as a function of temperature up to the isotropic state that may be indicative of significant change in the state of complexation.[40]

DSC analysis of the equimolar LC-1,*n*N/PAA mixtures shows the presence of a major transition within 2 or 3 °C of the melting point of pure LC-1,*n*N (as well as lower temperature minor transitions), and, in most cases, a new weak transition at higher temperature.[22] These transitions are plotted in Figure 6 as a function of alkyl spacer length. The enthalpies of the transition near 80 °C are consistently lower in the mixtures compared to those of the corresponding mesogen melting point (roughly by half when adjusted to the mesogen content, in most cases). Moreover, X-ray diffraction data in the temperature range below the dominant transition are essentially identical to those of the pure LC-1,*n*N, giving

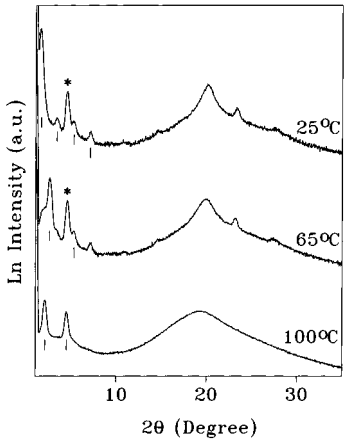

Figure 7. X-ray diffractograms of the equimolar LC-1,11N/PAA mixture at the nominal temperatures indicated, taken in order of decreasing temperature.

two distinct sets of profiles above and below the minor transitions (with the longer mesogens distinct from the shorter ones at ambient temperature), as well as having similar lamellar spacings (Figure 4, filled symbols) and similar intercepts and slopes of the Bragg distance vs *n* plots (Table 1). Typical profiles at temperatures below and above the minor transition are shown in Figure 7 (two lowest temperatures) for the LC-1,11N/PAA mixture, where the appropriate small-angle reflections for each phase are marked by vertical lines (noting that the 65 °C curve shows an overlap of the ambient temperature phase with the higher-temperature phase; see below for the peak marked with a asterisk).

Those data, along with the infrared results, are clearly indicative of the uncomplexed mesogens forming a separate phase from the complex. That the characteristics of this phase are unperturbed by the presence of the polymer or complex indicates that it is a mesogen-pure phase. By contrast, in mixtures of a carboxylic acid-terminated mesogen and poly(vinylpyridine), where only about 20% of the mesogens are complexed to the polymer by hydrogen bonds, the thermal characteristics of the mesogen phase are modified from those of the pure mesogen, suggesting a mesogen-rich rather than a mesogen-pure phase in that case.[27]

The new higher temperature transition (not apparent for $n = 6$ and barely for $n = 5$), which is weak (with enthalpies of about 1 kJ/mol) and sometimes quite broad, tends to increase rather strongly in temperature with an increase in spacer length (Figure 6), an effect that was also observed for the smectic A−isotropic transition in small-molecule liquid crystals with ionic mesogenic cores.[41] In POM, the samples are birefringent with an ill-defined small-grained texture (with no change after lengthy annealing), a typical example of which is shown in Figure 8. The birefringence generally disappears rather slowly (and reversibly) in the region of the DSC transition. The samples are highly viscous with significant elastic character above the mesogen melting point, remaining so up to high temperatures even in the isotropic phase. However, the initially separate powder grains clearly consolidate into a coherent sample as soon as the melting point is attained. These observations are consistent with the presence of a disordered liquid crystalline phase resulting from the formation of a polymer−mesogen complex and that coexists with the pure mesogen phase. An image of the biphasic character of the mixtures at ambient temper-

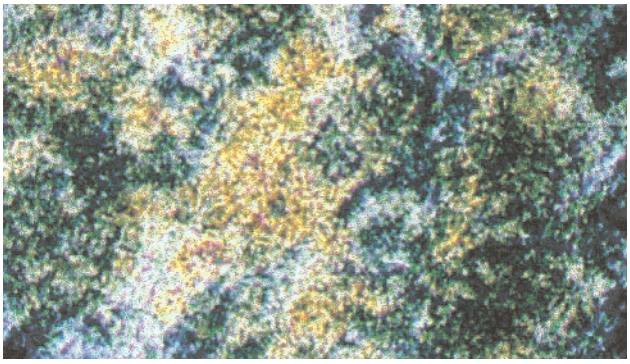

Figure 8. Polarizing optical micrograph of the equimolar LC-1,12N/PAA mixture at 120 °C (sample of nonuniform thickness).

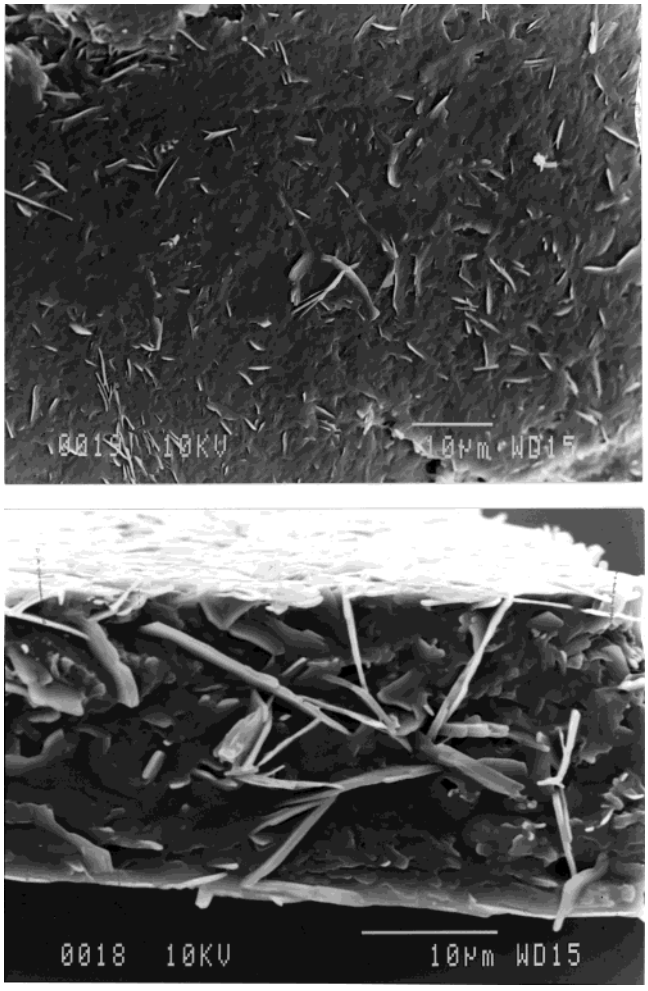

Figure 9. Scanning electron micrographs of two different areas of an equimolar LC-1,10N/PAA mixture.

ature (not evident in POM) is provided by the electron micrographs shown in Figure 9 for an equimolar LC-1,10N/PAA sample: platelike structures (where the ordered lamellar phase of pure LC-1,10N is presumably concentrated) are dispersed and embedded in an amorphous-looking matrix (which is presumably dominated by the complex).

It should be mentioned that when about 140 °C is exceeded, where PAA is reported to undergo anhydride reactions,[18,19,42] the clearing temperature tends to decrease somewhat on subsequent scans (observed, in particular, for $n = 12$; thus, the clearing temperature reported for this sample is that obtained on the first scan). This may be a consequence of the fewer number of available complexation sites on the polymer chain, leading to reduced complexation, or of the anhydride rings acting as impurities. Moreover, it was noted that the clearing temperature is somewhat less easily reproducible than the melting point, suggesting that the maximum amount of complexation attainable is sensitive to specific experimental/environmental details (although, as mentioned above, we were unable to establish a correlation between this and the variations observed in the infrared spectra). It may be added that no glass transitions were detected in the (equimolar) mixtures studied.

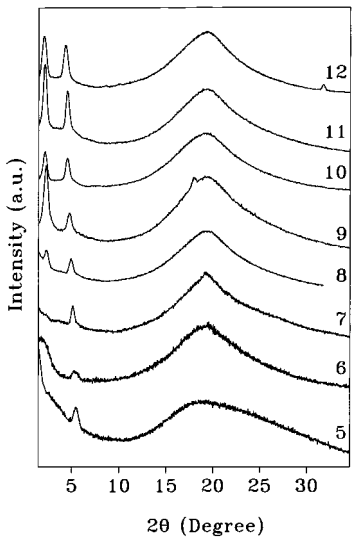

Figure 10. X-ray diffractograms of the equimolar LC-1,*n*N/PAA mixtures at about 90 °C for $n = 5-8$ and about 100 °C for $n = 9-12$ (the occasional weak peaks in the wide-angle region are artifacts).

X-ray diffractograms of the disordered birefringent phase are shown for LC-1,11N/PAA in Figure 7 (highest temperature curve) and for all of the mixtures in Figure 10. They are characterized by a broad peak located with its maximum at $2\theta = 19.7°$ ($d = 4.5$ Å) and, for $n > 7$, by two diffraction peaks at smaller angles with reciprocal spacings in the ratio 1:2. This is consistent with a disordered lamellar mesophase of the smectic A or C type. For $n = 5-7$, the reflection near $2\theta = 5-6°$ may be the second-order peak: not only does this peak continue to increase slightly in angle with a decrease in n, in continuity with the second-order peak of the other LC-1,*n*N/PAA, but also the indistinctness of a first-order peak in these mesogens is possibly related to the above-noted observation that the second-order peak is much more intense than the first-order one in the ambient temperature phase of the shorter mesogens (if it is a first-order reflection, then the Bragg spacing is less than one extended molecular length, which would be indicative of a tilted mesophase). The differences for the shorter compared to the longer mesogens may also be related to the greater difficulty of observing a mesophase−isotropic transition in DSC for the same mesogens, and may indicate that the spacer length is becoming too short to permit the adequate decoupling between the biphenyl core and the interacting diethylamine−polymer acid functionalities that may be necessary for well-defined lamellar ordering in these systems.

The lamellar spacings of the disordered mesophase as a function of n are shown by the filled circles in

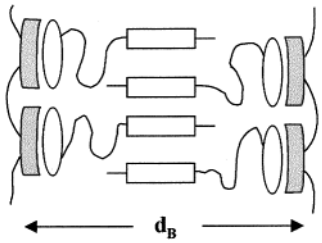

Figure 11. Simplified schematic representing the liquid crystalline phase of the LC-1,*n*N/PAA complexes.

Figure 4 (assuming that the peak for $n = 5-7$ is second-order). It is observed that they lie between one and two molecular lengths, indicative of a partial or interdigitated bilayer or a tilted bilayer. The ratio d/l is 1.33 ± 0.07 (based on the second-order reflection), with a slight tendency to decrease with increasing n; this d/l value is close to the value of 1.4 that is typical of orthogonal partial bilayer phases.[43] It may be remarked that partial or interdigitated bilayers are commonly observed for polymeric versions of low molar mass mesogens (specifically those with nonpolar tails) that present monolayer mesophases.[44] Tal'roze et al. also proposed an interdigitated model for the disordered lamellar mesophase in the analogous complexes of dimethylamine-functionalized molecules with PAA.[14] The lamellar spacing in our complexes increases with n at a rate of 1.4 Å/CH_2 and extrapolates to about 25 Å at $n = 0$ (Table 1). The molecular area, S, derived from the slope ($S = 2V_{CH_2}$/slope, where V_{CH_2} is the volume of one methylene group and is equal to 27.4 Å^3 at 70 °C[10,11]) is about 40(±6) Å^2; this compares favorably to (i.e., is reasonably larger than) the 30 Å^2 obtained in a smectic A phase of a protonated dimethylamine-capped surfactant−poly(vinyl sulfonate) complex and attributed to the size of the ammonium group.[11]

It was noted that the second-order (but not first-order) mesophase peak is generally visible in the profiles taken at temperatures below the melting point (see the peak marked with an asterisk in Figure 7). Its presence is consistent with the simultaneous existence of the liquid crystalline phase of the supramolecular complex that does not crystallize and the crystalline mesogen-pure phase. This reflection tends to move to somewhat smaller Bragg spacings with decreasing temperature, at least for the shorter mesogens (by as much as about 0.035 Å/°C, judging from the limited number of temperatures investigated). Such behavior is usually associated with tilted mesophases. It was also observed by Tal'roze et al. for their complexes, but only in a temperature range *above* a T_g ascribed to the complex; however, X-ray diffraction of oriented samples indicated that the mesophase is orthogonal in nature.[14] Preliminary data on an oriented nonequimolar LC-1,12N/PAA sample (0.4:1 amine:acid molar ratio) suggest that the mesophase in our complexes is also orthogonal.[16]

The above data for the disordered mesophase can be reconciled by the model in Figure 11, assuming an orthogonal phase. The mesogenic cores are shown to be interdigitated and the alkyl spacers highly disordered to maximize space-filling over an effective lateral area corresponding to that of about two mesogenic cores. This lateral area is also similar to that of the ammonium headgroup as estimated above. The compaction of the alkyl spacers along the layer normal is consistent with the value of the slope of d vs n. The extrapolated value for $n = 0$ then corresponds essentially to the length of the overlapped biphenyl core sublayer plus the amine−polymer backbone sublayer.

Conclusions

Equimolar mixtures of diethylamine-functionalized biphenyl mesogens and poly(acrylic acid) result in a biphasic system composed of a mesogen-pure phase and a phase composed of a supramolecular mesogen−polymer complex. The thermal and structural characteristics of the former are identical to those of the mesogens alone: they melt from a lamellar E-like phase to the isotropic phase at about 80 °C independently of the spacer length, and generally possess at least two lamellar crystalline or ordered phases, one of which is a monolayer and the other a (partial) bilayer with details depending on the spacer length. The mesogen−polymer complex is a result of proton transfer from the acid to amine groups, leading to complementary (hydrogen-bonded) ion pairs—or strong proton polarization—binding the two components, and appears to involve approximately half of the mesogens in the equimolar mixtures. The complex forms a disordered liquid crystalline mesophase, most likely an orthogonal partial or interdigitated (smectic A) bilayer. It is stable to higher temperatures than the ordered LC-1,*n*N phase, and the smectic−isotropic transition temperature increases strongly with spacer length. In terms of its biphasic character and the nature of the complex, the LC-1,*n*N/PAA system behaves qualitatively similarly to analogous systems reported in the literature,[14] showing that this behavior is qualitatively independent (within the limited range of molecular parameters studied) of the amine substituents (methyl or ethyl), the spacer length ($n = 2$ in ref 14), and the mesogenic moiety [short or longer core, short or long (para-substituted) alkyl tail]. On the other hand, the obtention of a well-defined liquid crystalline phase for the $n = 2$ system[14] compared to the apparently greater difficulty for the shorter mesogens of this study is possibly related to the dimethylamine vs diethylamine functionalities: the larger head size of the latter may be less commensurate with the molecular area of the mesogenic core and therefore require greater decoupling for well-defined mesophase formation. It is also possible that the effects of the very short spacer are compensated by the long alkyl tail in the $n = 2$ system.

Acknowledgment. Acknowledgement is made to the donors of the Petroleum Research Fund, administered by the American Chemical Society, for partial support of this research. NSERC (Canada) and FCAR (Québec) are acknowledged for additional financial support. A.T. thanks the Ministry of Science and Higher Education of the Islamic Republic of Iran for a Ph.D. scholarship. We are grateful to H. Tremblay (now at Biosyntech) for contributing some experimental verifications and to R. Bissessur (now at the University of Prince Edward Island) for obtaining the electron micrographs.

Supporting Information Available: Text describing the synthesis of the LC-1,*n*N, a table of their elemental analyses, DSC thermograms of the pure LC-1,*n*N and their mixtures with PAA, and a table of the associated transition temperatures and enthalpies. This material is available free of charge via the Internet at http://pubs.acs.org.

References and Notes

(1) Bazuin, C. G. In *Mechanical and Thermophysical Properties of Polymer Liquid Crystals*; Brostow, W., Ed.; Chapman and Hall: London, 1998; Vol. 3, Chapter 3.

(2) Kato, T.; Fréchet, J. M. J. *Macromol. Symp.* **1995**, *98*, 311. Kato, T. In *Handbook of Liquid Crystals*; Demus, D., Goodby, J. W., Gray, G. W., Spiess, H. W., Vill, V., Eds.; Wiley-VCH: Weinheim, 1998; Vol. 2B, p 969.

(3) Tal'roze, R. V.; Kuptsov, S. A.; Lebedeva, T. L.; Shandryuk, G. A.; Stepina, N. D. *Macromol. Symp.* **1997**, *117*, 219. Tal'roze, R. V.; Kuptsov, S. A.; Sycheva, T. I.; Shandryuk, G. A.; Platé, N. A. *Am. Chem. Soc. Symp. Ser.* **1996**, *632*, 304.

(4) For example see: Lee, C.-M.; Jariwala, C. P.; Griffin, A. C. *Polymer* **1994**, *35*, 4550. St. Pourcain, C. B.; Griffin, A. C. *Macromolecules* **1995**, *28*, 4116.

(5) Fouquey, C.; Lehn, J.-M.; Levelut, A.-M. *Adv. Mater.* **1990**, *2*, 254.

(6) For example see: Kato, T.; Fréchet, J. M. J. *Macromolecules* **1989**, *22*, 3818. Kato, T.; Kihara, H.; Uryu, T.; Fujishima, A.; Fréchet, J. M. J. *Macromolecules* **1992**, *25*, 6836. Kato, T.; Kihara, H.; Ujiie, S.; Uryu, T.; Fréchet, J. M. J. *Macromolecules* **1996**, *29*, 8734.

(7) For example see: Ruokolainen, J.; ten Brinke, G.; Ikkala, O.; Torkkeli, M.; Serimaa, R. *Macromolecules* **1996**, *29*, 3409. Ruokolainen, J.; Torkkeli, M.; Serimaa, R.; Vahvaselka, S.; Saariaho, M.; ten Brinke, G.; Ikkala, O. *Macromolecules* **1996**, *29*, 6621. Ruokolainen, J.; Saariaho, M.; Ikkala, O.; ten Brinke, G.; Thomas, E. L.; Torkkeli, M.; Serimaa, R. *Macromolecules* **1999**, *32*, 1152.

(8) For example see: Antonietti, M.; Conrad, J.; Thünemann, A. *Macromolecules* **1994**, *27*, 6007. Antonietti, M.; Burger, C.; Conrad, J.; Kaul, A. *Macromol. Symp.* **1996**, *106*, 1.

(9) For example see: Ponomarenko, E. A.; Waddon, A. J.; Bakeev, K. N.; Tirrell, D. A.; MacKnight, W. J. *Macromolecules* **1996**, *29*, 4340. Ponomarenko, E. A.; Tirrell, D. A.; MacKnight, W. J. *Macromolecules* **1998**, *31*, 1584.

(10) Tsiourvas, D.; Paleos, C. M.; Skoulios, A. *Macromolecules* **1997**, *30*, 7191.

(11) Tsiourvas, D.; Paleos, C. M.; Skoulios, A. *Macromolecules* **1999**, *32*, 8059.

(12) Ujiie, S.; Iimura, K. *Macromolecules* **1992**, *25*, 3174.

(13) Bazuin, C. G.; Tork, A. *Macromolecules* **1995**, *28*, 8877.

(14) Tal'roze, R. V.; Kuptsov, S. A.; Sycheva, T. I.; Bezborodov, V. S.; Platé, N. A. *Macromolecules* **1995**, *28*, 8689.

(15) Kawakami, T.; Kato, T. *Macromolecules* **1998**, *31*, 4475.

(16) A separate paper on nonstoichiometric mixtures is in preparation.

(17) Kornienko, E. V.; Sycheva, T. I.; Kuptsov, S. A.; Bezborodov, V. S.; Lebedeva, T. L.; Tal'roze, R. V.; Platé, N. A. *Polym. Sci.* **1992**, *34*, 997.

(18) Eisenberg, A.; Yokoyama, T.; Sambalido, E. *J. Polym. Sci., Part A-1* **1969**, *7*, 1717.

(19) Maurer, J. J.; Eustace, D. J.; Ratcliffe, C. T. *Macromolecules* **1987**, *20*, 196.

(20) Dong, J.; Ozaki, Y.; Nakashima, K. *Macromolecules* **1997**, *30*, 1111.

(21) It was noted, however, that, after some time of storage, the samples did tend to show some birefringence to well above the melting point, in the form of rigid crystalline-like islands in a fluid liquid. This may be caused by protonation of some proportion of the amine moieties by water molecules. This effect appears to influence the melting point only slightly, namely, to the extent indicated by the variation in temperature as a function of spacer length. Br-terminated samples similarly became birefringent in the melt after long-term storage, which was eliminated by recrystallization.

(22) See the Supporting Information for the DSC thermograms and associated transition temperatures and enthalpies.

(23) Tremblay, H. M. Sc. Thesis, Chemistry Department, Laval University, Quebec, 2000.

(24) Recommended IUPAC nomenclature for the formerly designated smectic E mesophase; document in preparation (M. Biron, private communication).

(25) Gray, G. W.; Goodby, J. W. *Smectic Liquid Crystals, Textures and Structures*, Leonard Hill: Glasgow, Scotland, 1984; plate 33. The texture shown in the reference was obtained by cooling from a homeotropic smectic A phase.

(26) There is discussion as to whether the E phase is always truly crystalline. See, for example, ref 10 about possible "hexatic" E phases.

(27) Brandys, F. A.; Bazuin, C. G. *Chem. Mater.* **1996**, *8*, 81.

(28) Koltzenburg, S.; Wolff, D.; Springer, J.; Nuyken, O. *J. Polym. Sci., Part A: Polym. Chem.* **1998**, *36*, 2669.

(29) Navarro-Rodriguez, D.; Frère, Y.; Gramain, P.; Guillon, D.; Skoulios, A. *Liq. Cryst.* **1991**, *9*, 321. Navarro-Rodriguez D.; Guillon, D.; Skoulios, A.; Frère, Y.; Gramain, Ph. *Macromol. Chem.* **1992**, *193*, 317.

(30) Demus, D.; Richter, L.; Rürup, C.-E.; Sackmann, H.; Schubert, H. *J. Phys. (Paris), Colloq.* **1975**, *36*, C1−349.

(31) Under some circumstances (not determined in detail), the ambient temperature phase for $n = 8$ is the same as that obtained for the longer mesogens. Furthermore, for $n = 9$, a transition from the higher temperature phase (middle curve of Figure 3b) to a phase similar to that of the shorter mesogens at ambient temperature (third and second curves from the top of Figure 3b) was detected between 70 and 65 °C in a series of X-ray measurements obtained on cooling; this was followed by another transition near 60 °C to the ambient temperature phase of the longer mesogens (top curve of Figure 3b, and partly visible in the second curve from the top). This is probably a cause of the presence of more than one minor transition in the DSC thermograms.

(32) Ujiie, S.; Takagi, S.; Sato, M. *High Perform. Polym.* **1998**, *10*, 139.

(33) See, for example, the review: Tschierske, C. *Prog. Polym. Sci.* **1996**, *21*, 776 and references therein.

(34) Barbarin, F.; Dugay, M.; Piovesan, A.; Fadel, H.; Guillon, D.; Skoulios, A. *Liq. Cryst.* **1987**, *2*, 815. Fadel, H.; Guillon, D.; Skoulios, A.; Barbarin, F.; Dugay, M. *J. Phys. (Paris)* **1989**, *50*, 375.

(35) Gavril, M. M. Sc. Thesis, Chemistry Department, Laval University, Quebec, 1995.

(36) Pasto, D. J.; Johnson, C. R. *Organic Structure Determination*; Prentice Hall: Englewood Cliffs, NJ, 1969.

(37) Brozoski, B. A.; Coleman, M. M.; Painter, P. C. *Macromolecules* **1984**, *17*, 230.

(38) Lebedeva, T. L.; Shandryuk, G. A.; Sycheva, T. I.; Bezborodov, V. S.; Tal'roze, R. V.; Platé, N. A. *J. Mol. Struct.* **1995**, *354*, 89.

(39) Brandys, F. A.; Masson, P.; Guillon, D.; Bazuin, C. G. *Macromol. Chem. Phys.* **2001**, *202*, 856.

(40) Tremblay, H.; Pézolet, M.; Bazuin, C. G. Manuscript in preparation.

(41) Tabrizian, M.; Soldera, A.; Couturier, M.; Bazuin, C. G. *Liq. Cryst.* **1995**, *18*, 475 and references therein.

(42) An infrared spectrum of one of the complexes heated to above 140 °C indeed confirmed the presence of a small amount of anhydride carbonyl.

(43) Gray, G. W.; Goodby, J. W. *Smectic Liquid Crystals, Textures and Structures*; Leonard Hill: Glasgow, Scotland, 1984.

(44) Keller, E. N. *Macromolecules* **1989**, *22*, 4597.

MA010607F